NASA TECHNICAL NOTE

EXPERIMENTAL INVESTIGATION OF
HEAT TRANSFER AND PRESSURES
ON A SWEPT CYLINDER IN THE VICINITY
OF ITS INTERSECTION WITH A WEDGE AND
FLAT PLATE AT MACH NUMBER 4.15
AND HIGH REYNOLDS NUMBERS

by Ivan E. Beckwith

Langley Research Center
Langley Station, Hampton, Va.

EXPERIMENTAL INVESTIGATION OF HEAT TRANSFER AND PRESSURES

ON A SWEPT CYLINDER IN THE VICINITY OF ITS INTERSECTION

WITH A WEDGE AND FLAT PLATE AT MACH NUMBER 4.15

AND HIGH REYNOLDS NUMBERS

By Ivan E. Beckwith

Langley Research Center
Langley Station, Hampton, Va.

NATIONAL AERONAUTICS AND SPACE ADMINISTRATION

NATIONAL AERONAUTICS AND SPACE ADMINISTRATION

TECHNICAL NOTE D-2020

EXPERIMENTAL INVESTIGATION OF HEAT TRANSFER AND PRESSURES

ON A SWEPT CYLINDER IN THE VICINITY OF ITS INTERSECTION

WITH A WEDGE AND FLAT PLATE AT MACH NUMBER 4.15

AND HIGH REYNOLDS NUMBERS

By Ivan E. Beckwith

SUMMARY

Heat-transfer rates and pressures have been measured on a circular cylinder in the region of flow interference caused by an adjoining 8° half-angle sharp wedge. Data were obtained at sweep angles of 20° and 60° with respect to the free-stream flow direction. At the 20° sweep angle some data were obtained with a flat plate as well as with the wedge. The test Reynolds numbers were sufficiently large so that the boundary layer was always turbulent on the cylinder and wedge or plate.

For 20° sweep angle the peak values of pressure and heat transfer occurred about half a cylinder diameter from the wedge and were apparently caused by local flow conditions and separation on the wedge upstream of the cylinder. When the sweep angle was 60°, no separation occurred, and the peak pressure and heat transfer on the cylinder could be accurately predicted by the theory for turbulent heating on a yawed cylinder from the local flow conditions on the wedge. The local effect on the heating rates of the shock-wave impingement from the wedge was negligible at both sweep angles.

INTRODUCTION

The local aerodynamic heating rates and pressures on simple shapes may be altered considerably when the flow field or boundary layer is modified by an adjoining body. Similar variations in heating and pressures can be expected in the interference region between wings and bodies, control surfaces and supporting structures, or any other adjacent parts that may be found on high-velocity vehicles.

Some early data illustrating an interference effect were given in reference 1 (originally published in 1958), wherein turbulent heating rates were observed at the stagnation line of a cylindrical leading edge at zero sweep. The data were obtained about 1 inch from the root of the wing leading-edge segment, which was

mounted approximately midway on a 76.6-inch-long pointed body of revolution. Since turbulent flow is not expected at the stagnation line of an unswept infinite cylinder, it is apparent that in this case the flow field and boundary layer about the body of revolution were responsible for causing turbulent flow on the cylinder. Presumably, the bow shock from the cylinder would cause upstream separation of the flow on the body, with the result that a spanwise flow component could be generated on the cylinder. The cylinder would, in effect, be at some sweep angle, and for the test conditions (Mach numbers up to 3 and leading-edge Reynolds numbers up to 1.2×10^6), turbulent flow could then exist along the leading edge. It has been shown in references 2 and 3, for example, that transition to turbulent flow on swept leading edges can be expected at comparatively low Reynolds numbers. In the data of reference 1, the bow shock from the body does not affect the results, since the wing stub was submerged in the body flow field.

In another investigation (ref. 4) detailed studies were made of interference effects on heating and pressures on a flat plate and on various protuberances mounted on the plate. (Pressure data on the protuberances were not obtained.) Included among these protuberances were circular cylinders at 0° and 45° sweep with respect to the plate and free-stream flow. The heating rates at the stagnation line of the cylinders at both sweep angles were up to three times larger than the undisturbed laminar values. In view of the Reynolds number range of the tests (up to about 1×10^6 based on cylinder diameter), the explanation for the increased heating is probably the same as that proposed herein for the similar increases observed in reference 1. In both cases, however, the lack of schlieren and pressure data makes quantitative analysis uncertain.

In references 1 and 4 the bow shock generated by the supporting body or plate was outside the region on the leading edge that was investigated. In references 5, 6, and 7 the test models were constructed so that the shock wave would impinge on the instrumented region of the leading edge. In the investigation of reference 5, a $16\frac{1}{4}^o$ wedge and an unyawed circular cylinder were mounted in tandem on a flat plate. The shock generated by the wedge, as well as the wedge flow field and separation at the base of the cylinder, probably contributed indirectly to the increased stagnation-line heating, which was up to three times larger than the corresponding laminar values on an undisturbed cylinder. Although no comparisons with turbulent-heating estimates were made in reference 5, it can be shown that if local conditions upstream of the cylinder are accounted for properly, the reported peak values are in reasonable agreement (both as to level and trend with Mach number) with the turbulent theory of reference 2.

In reference 6 a blunt slab with a circular leading edge was mounted on a flat plate alined with the free stream. A weak shock from the plate leading edge impinged on the slab leading edge, which was swept back 60°. At the largest Reynolds number of these tests, the leading-edge heating was about three times the undisturbed laminar value. Comparison of the data with turbulent theory for yawed cylinders indicated that the increased heating was caused by transition to turbulent flow. Apparently the disturbances caused by the impinging shock, as well as flow separation at the root of the leading edge, were sufficient to cause transition.

2

In the investigation of reference 7, the heating was measured at the stagnation line of an unswept circular cylinder, which was mounted on a hemisphere-cylinder model of about the same diameter. The test cylinder was only about 2 diameters downstream of the nose of the hemisphere-cylinder model and was thus strongly influenced by its flow field and bow shock. The heating rates at the measuring stations nearest the supporting body were generally the largest and varied from theoretical laminar to turbulent values. Farther outboard, in the shock-impingement region, the heating rates were less than theoretical laminar values except at the highest Mach and Reynolds numbers, where the data were between the predicted laminar and turbulent values. For these data the upper limit of the interference heating can again be predicted by turbulent theory.

The purpose of this report is to present additional data and analysis showing the interference effects of a wedge shock and flow field on pressures and heat transfer to a circular cylinder at sweep angles of 20° and 60°. The test Reynolds numbers were so large that completely turbulent boundary layer was observed, even for the undisturbed cylinder. The results are thus not affected by transition, and, in addition, the shapes employed allow a simplified analysis based on local flow conditions.

SYMBOLS

D	cylinder diameter (fig. 1)
h	heat-transfer coefficient, $\dfrac{q_W}{T_{aw} - T_W}$
h_{inf}	measured values of heat-transfer coefficients on infinite cylinder from reference 2
k	thermal conductivity
l	upstream length of flat plate or wedge from stagnation line of cylinder (fig. 1)
M	Mach number
p	pressure
q	heat-transfer rate
$R_{\infty,D}$	free-stream Reynolds number based on cylinder diameter, $\dfrac{\rho_\infty u_\infty D}{\mu_\infty}$
T	temperature
T_{aw}	local measured recovery temperature
u_∞	free-stream velocity

y   axial distance along surface of cylinder from wedge intersection line (fig. 1)

α wedge half-angle (or plate angle of attack) (fig. 1), deg

θ angular distance from stagnation line of cylinder, deg

Λ yaw or sweep angle of cylinder (see fig. 1)

μ viscosity

ρ density

Subscripts:

o   settling chamber (free-stream stagnation conditions)

s   stagnation line of cylinder

w   wall conditions

∞ free stream

APPARATUS AND TEST CONDITIONS

Tunnel

The tests were conducted in a blow-down tunnel over a nominal range of stagnation pressures and temperatures of 200 to 500 lb/sq in. gage and 150° F to 300° F. The Mach number in the test section was 4.15 ± 0.03. The free-stream Reynolds number based on cylinder diameter was varied from about 1.6×10^6 to 4.0×10^6. The nozzle and other test conditions such as coolant temperatures are the same as those of reference 2.

Model

A sketch of the configuration is shown in figure 1(a). As indicated in figure 1(b), all instrumentation was on one generatrix of the cylinder, which could be translated or rotated within the wedge. Data were obtained at yaw angles of 20° and 60° with two different wedges made for these angles. With the 8° half-angle wedge for $\Lambda = 20^\circ$, the upstream length l was 4.16 inches; whereas for $\Lambda = 60^\circ$, l was 3.28 inches. Some data were also obtained at $\Lambda = 20^\circ$ with flat plates instead of the wedge, that is, with $\alpha = 0^\circ$. The two plates used were made with values of l of 4.13 and 1.57 inches. The clearance space between the wedges and cylinder (or plates) was sealed with a gasket.
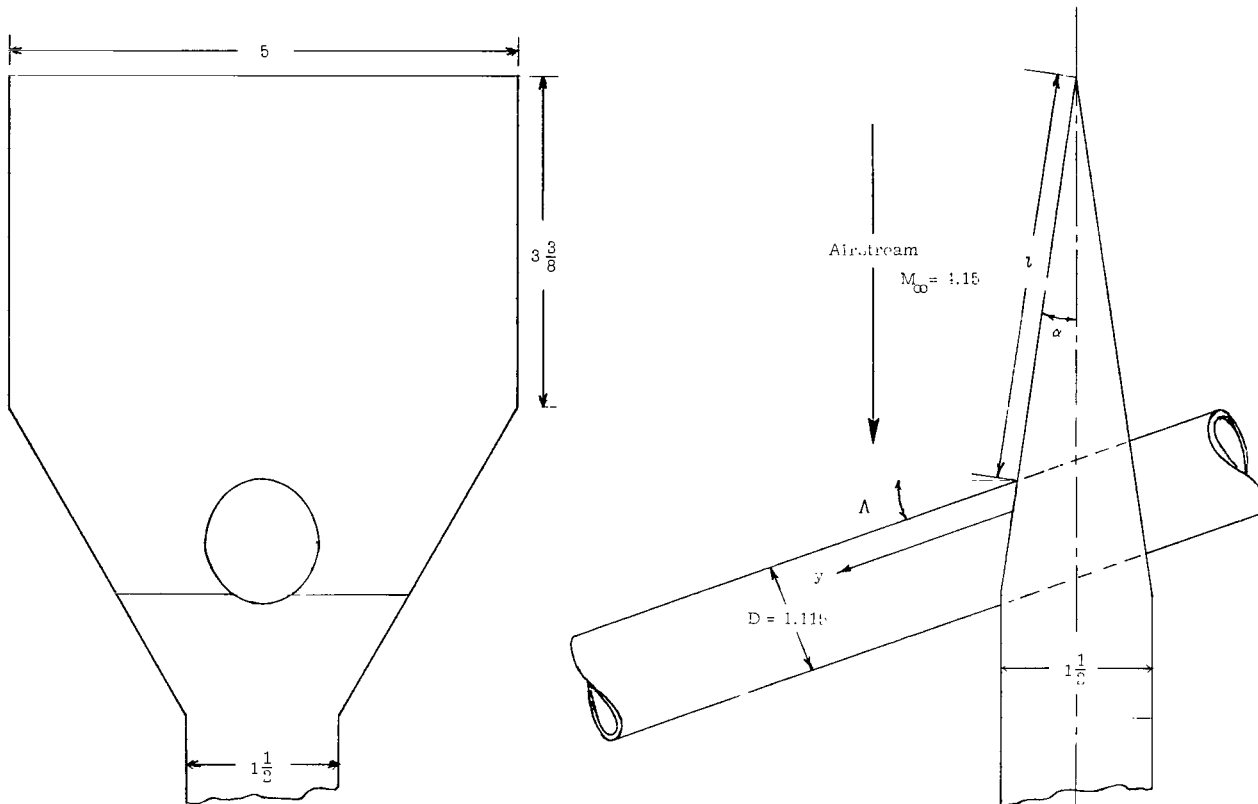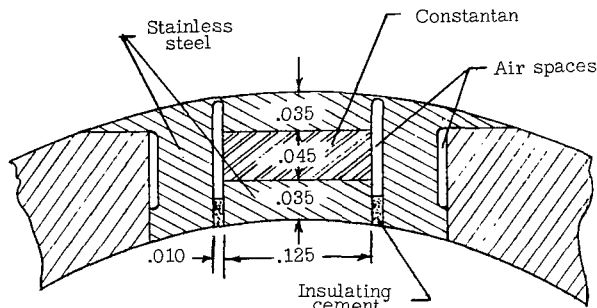
(a) Basic configuration.
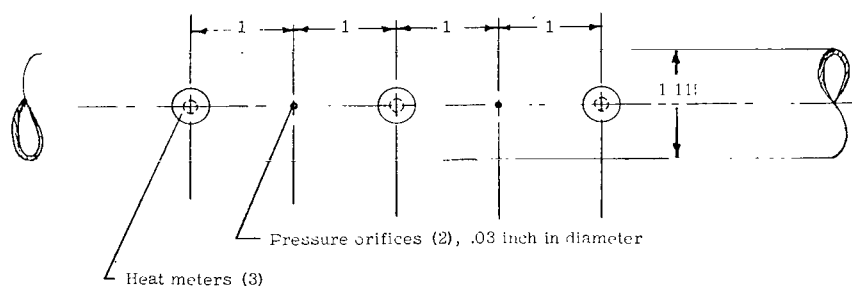
(b) Relative location of pressure orifices and heat meters.

Figure 1.- Sketch of model and instrumentation. (All dimensions in inches.)

The cylinder used in the present tests is the same as one used in reference 2 and was designated therein as the "second model." Heat-transfer rates were measured directly by means of heat meters after steady tunnel flow and coolant conditions were reached. Varsol was used as the coolant. A cross-sectional sketch of a heat meter is given in figure 1(c). The electromotive force, which is measured from the inside stainless steel disk to the outer stainless steel body, is proportional to the temperature drop across the constantan disk. The heat-transfer rate to the exterior surface of the model was then obtained from this temperature drop by application of suitable proportionality and correction factors (see ref. 2). Model pressures were measured with mercury manometers. A few

(c) Cross-sectional sketch of heat meter.

Figure 1.- Concluded.

pressure orifices were installed on the wedges and plates; however, since these were not in the interaction region, the results are not reported herein. Complete details of instrumentation and test procedures are given in reference 2.


RESULTS AND DISCUSSION

Pressures

$\Lambda = 20^{\circ}$.- Pressure distribution data on the cylinder at a yaw angle of 20° with the 8° half-angle wedge are shown in figure 2. All pressure data are presented as ratios of the local measured pressure to the measured tunnel stagnation or settling-chamber pressure. In figure 2(a) the pressure ratios are plotted against θ, the angular distance around the cylinder, at several spanwise stations. The distances of these spanwise stations from the wedge as measured along the stagnation line are designated y_s in the figure. The plane of the survey in θ is normal to the cylinder axis. For $y_s = 2.19$ and 3.69 inches the pressure distributions are nearly the same and can be assumed to represent the distribution on an undisturbed cylinder at a yaw angle of 20°, as indicated by comparison with the undisturbed stagnation-line pressure ratio of about 0.108 shown in the figure. (The data for $y_s = 3.69$ inches were used in ref. 2 as values for the undisturbed cylinder.) As the wedge is approached, the pressures over the forward portion of the cylinder increase until at $y_s = 0.44$ inch the stagnation-line pressure ratio is more than twice the undisturbed pressure ratio. This trend of increased pressures persists over the entire forward half of the cylinder and can be accounted for by local separation of the flow upstream of the cylinder on the face of the wedge.

The pressure ratio is plotted against the spanwise distance y in figure 2(b) for several values of θ and two Reynolds numbers. The sharp peak pressure at about 0.5 inch from the wedge is shown clearly in this figure. The

6
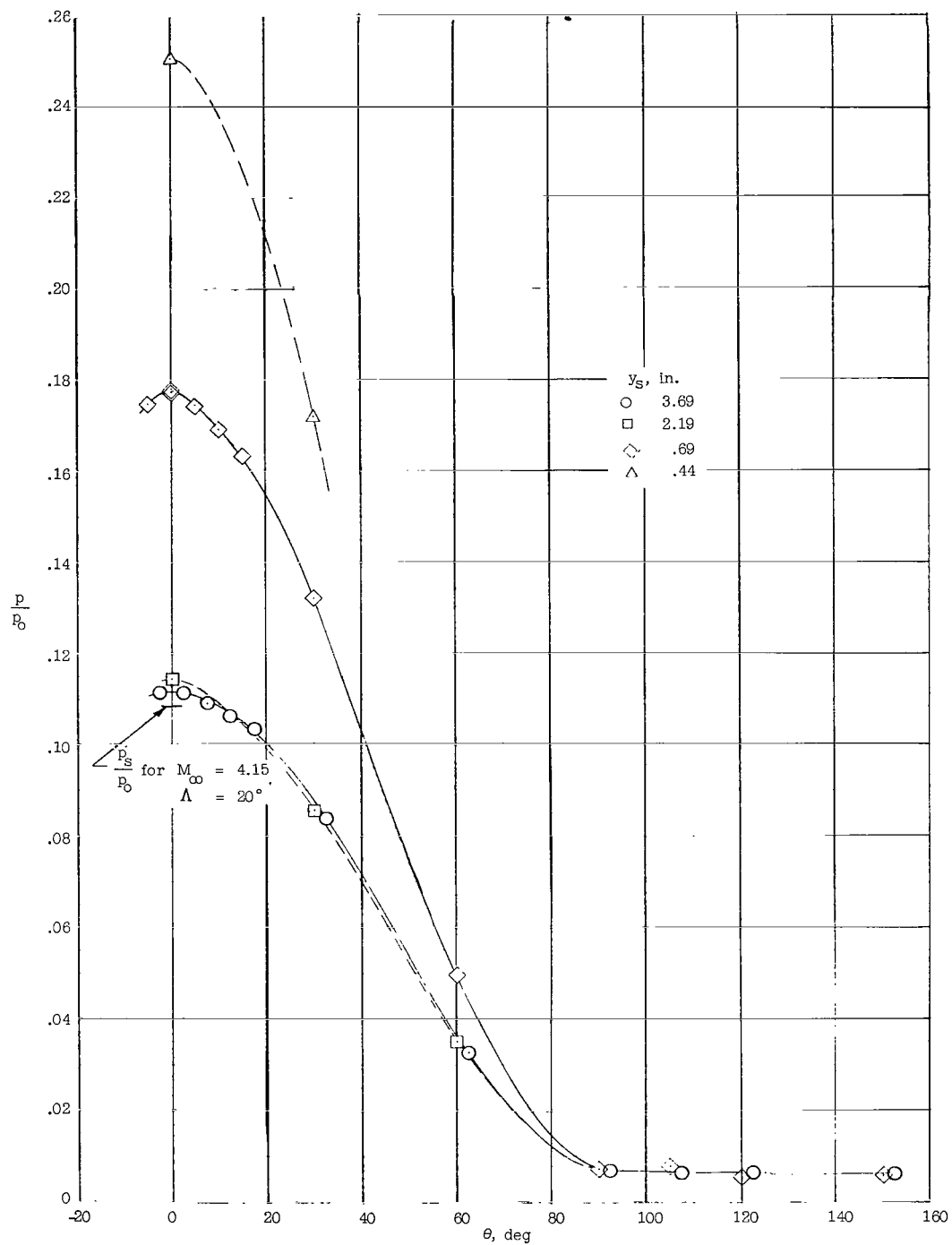
(a) Chordwise pressure distribution at four spanwise stations. $R_{\infty,D} = 1.97 \times 10^6$.

Figure 2.- Pressure distribution on cylinder for $\Lambda = 20°$, $\alpha = 8°$, and $l = 4.16$ inches.
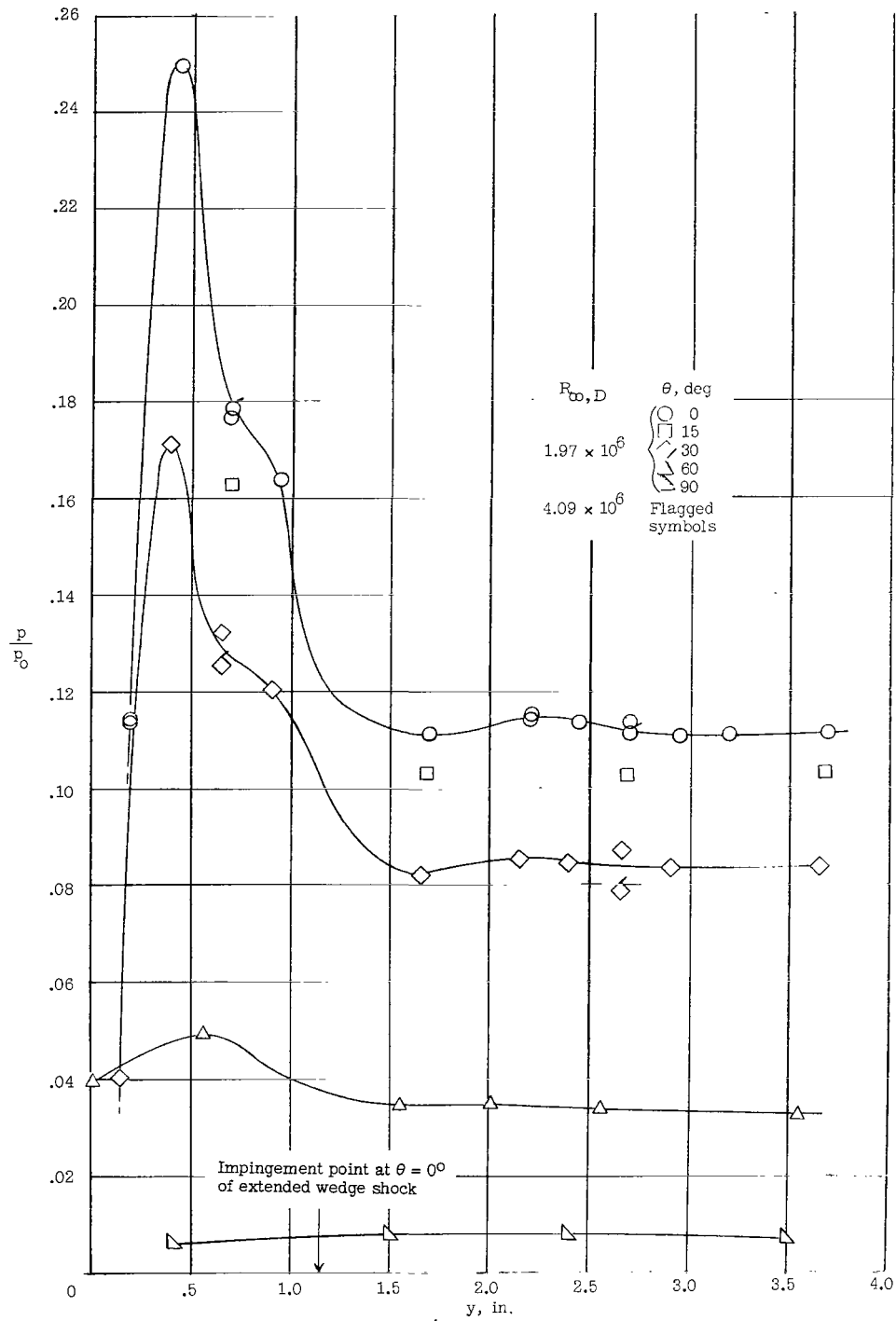
(b) Spanwise pressure distribution for several values of θ and two Reynolds numbers.

Figure 2.- Concluded.

8

large reduction in pressure very near the wedge provides further indication that a separated-flow region was present. If the wedge shock were extended with no change in angle, it would impinge on the cylinder leading edge at about $y_s = 1.15$ inches, as indicated in the figure. Note that the pressure disturbance is still small at this value of y_s. Also note that a change in Reynolds number from 1.97×10^6 to 4.09×10^6 had little effect on pressure ratios. This independence of Reynolds number would be expected if the wedge boundary layer were always turbulent.

Although no schlieren data are available at $\Lambda = 20^O$, the presence of separation can be shown by considering two extreme conditions. If it is first assumed that a shock is attached at the intersection line as indicated in figure 3, which is a sketch of the assumed flow pattern for $\Lambda = 20^O$, then the value of p_s/p_O on the cylinder in region ② would be about 0.18, with the exact value depending on the assumed shock-wave angle. On the other hand, if isentropic compression from the local wedge flow in region ① normal to the cylinder is assumed, the value of p_s/p_O would be about 0.50. Since the peak experimental value at the stagnation line is 0.25 (fig. 2(b)), intermediate between the aforementioned two extremes, it is apparent that some separation is present with a weak oblique shock (or series of shocks) extending forward on the wedge as depicted in figure 3.
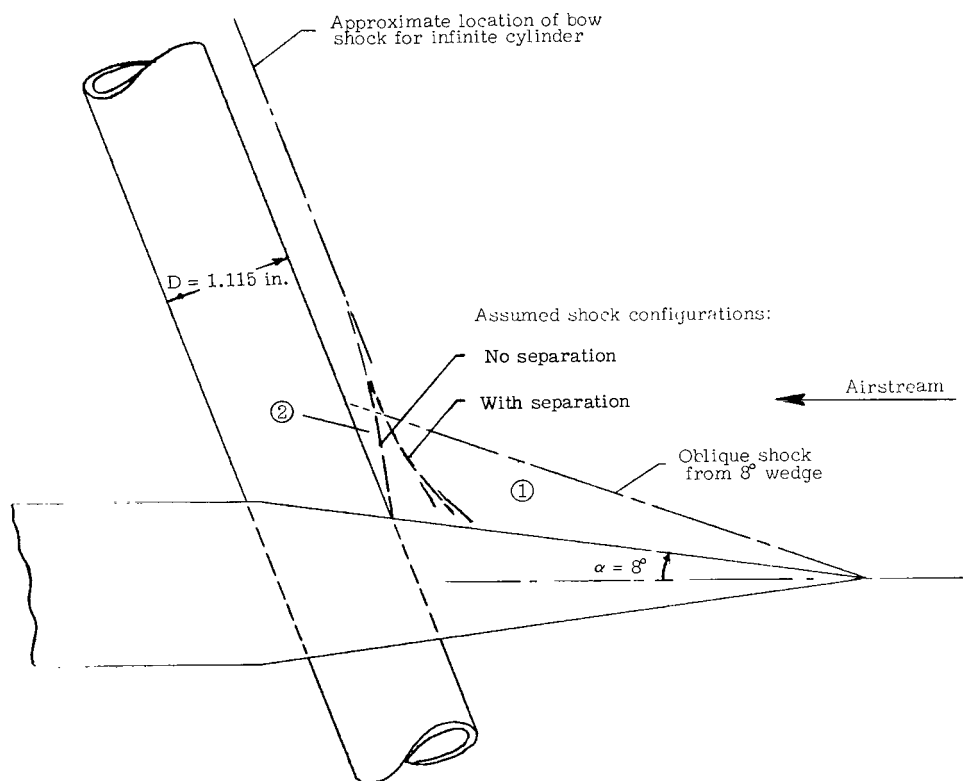

Figure 3.- Schematic flow sketch for $\Lambda = 20^O$.

The stagnation-line pressure distributions as obtained on the cylinder with the 8° half-angle wedge and with flat plates of two different lengths are compared in figure 4. The peak pressure with the shorter flat plate is considerably less
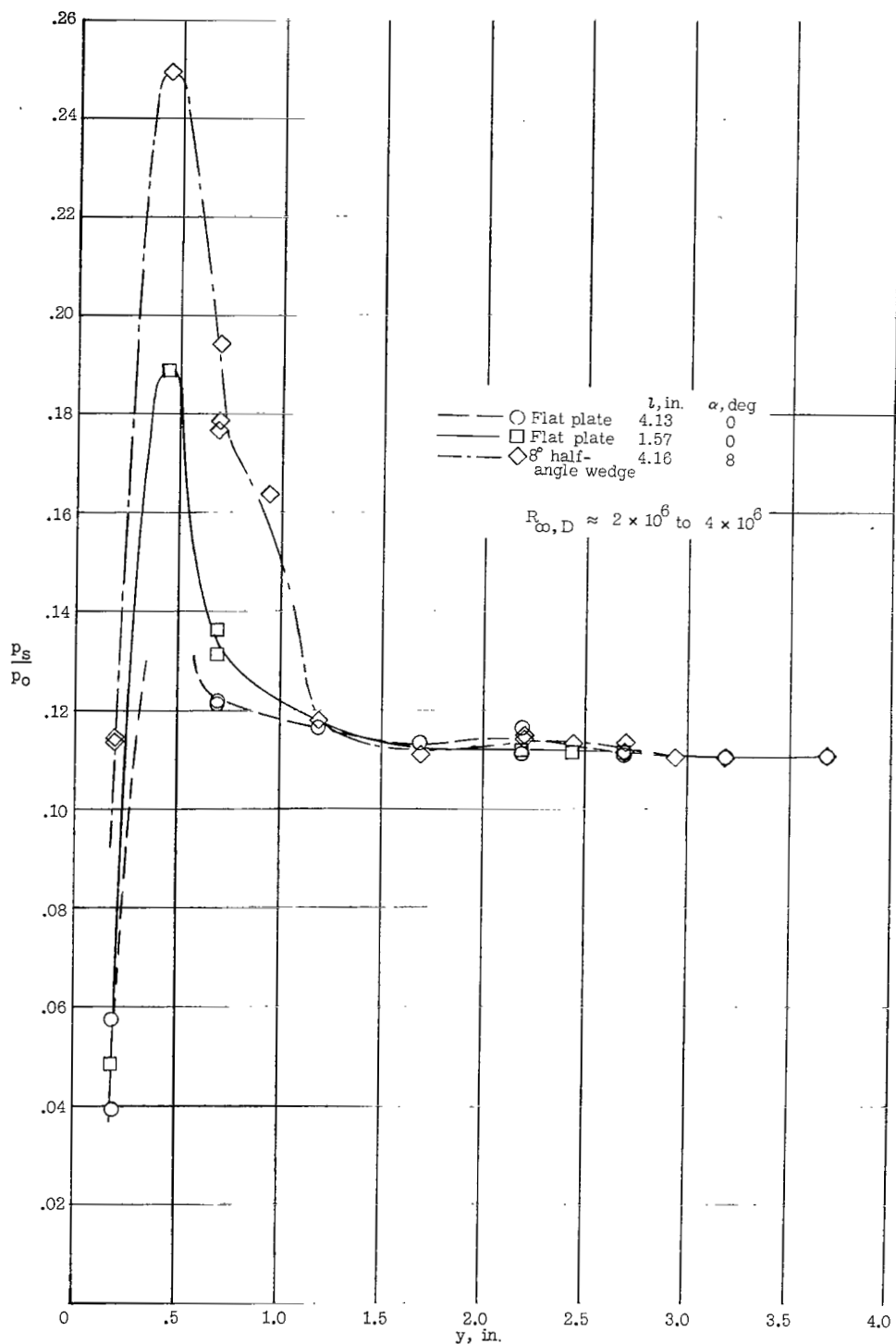

Figure 4.- Effect of wedge angle and length on spanwise pressure distribution at stagnation line of cylinder for $\Lambda = 20°$.

than the peak pressure with the wedge. The peak pressure with the longer flat plate was not obtained. (It should be noted that the peak pressures indicated by the faired lines in figs. 2(b) and 4 may not be exactly correct because of the limited number of experimental points available.) The smaller peak cylinder pressure observed with the flat plate as compared with that for the wedge evidently results from the fact that the flow passes through only one shock (or set of shocks) at the base of the cylinder. When the flow also traverses the wedge shock, the final stagnation pressure must be larger.

$\Lambda = 60^{\circ}$.- The pressure distribution on the cylinder at $\Lambda = 60^{\circ}$ with the 8° half-angle wedge is shown in figure 5. The pressure ratio is plotted against θ in figure 5(a), which shows that the pressure again increased as the wedge was approached, as was noted for $\Lambda = 20^{\circ}$ in figure 2. The effects appear to extend outward a greater y distance than for $\Lambda = 20^{\circ}$, since for $y_s = 4.25$ inches the pressures are still larger than those on a corresponding undisturbed cylinder represented by the circular symbols in figure 5(a). The pressure-ratio data are plotted against spanwise distance from the wedge intersection y in figure 5(b).
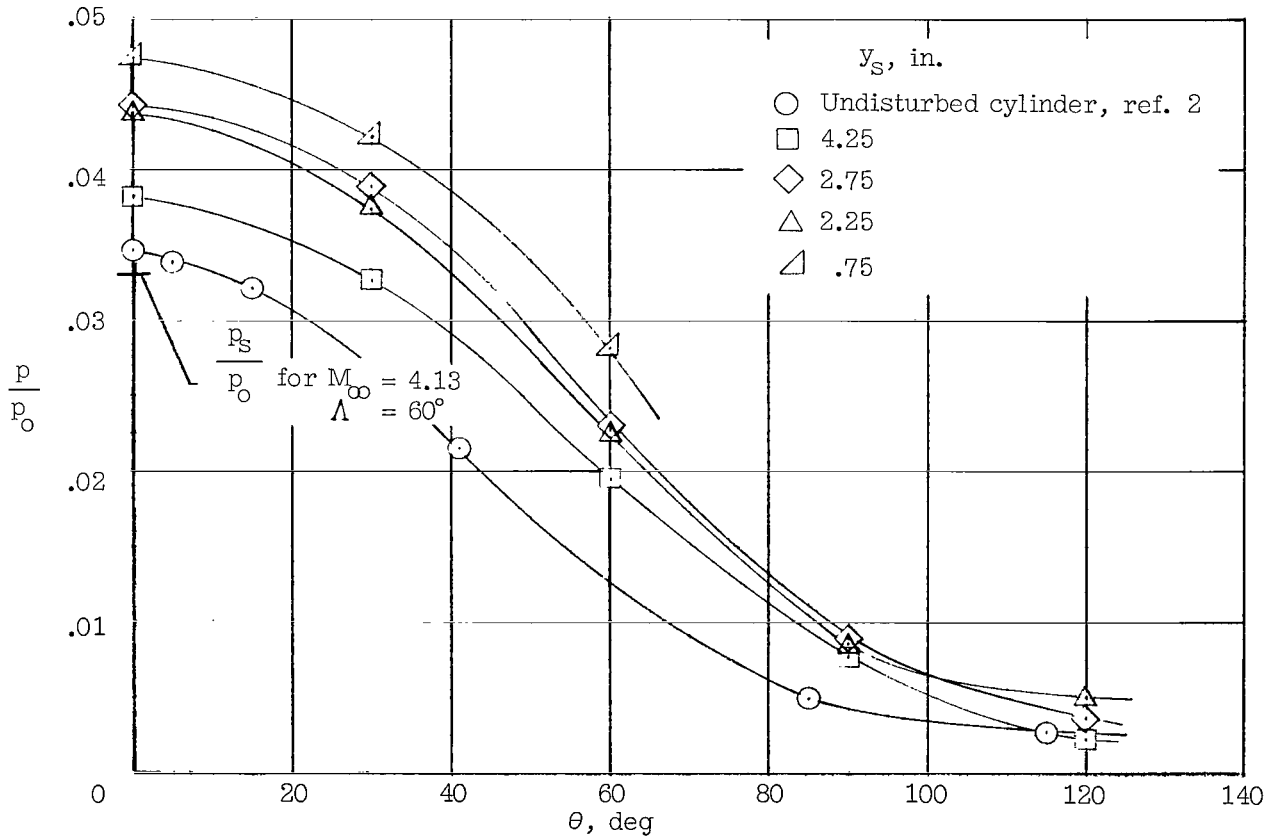
(a) Chordwise pressure distribution at several spanwise stations.

Figure 5.- Pressure distribution on cylinder with $\Lambda = 60^{\circ}$, $\alpha = 8^{\circ}$, $l = 3.28$ inches, and $R_{\infty,D} = 1.8 \times 10^6$.
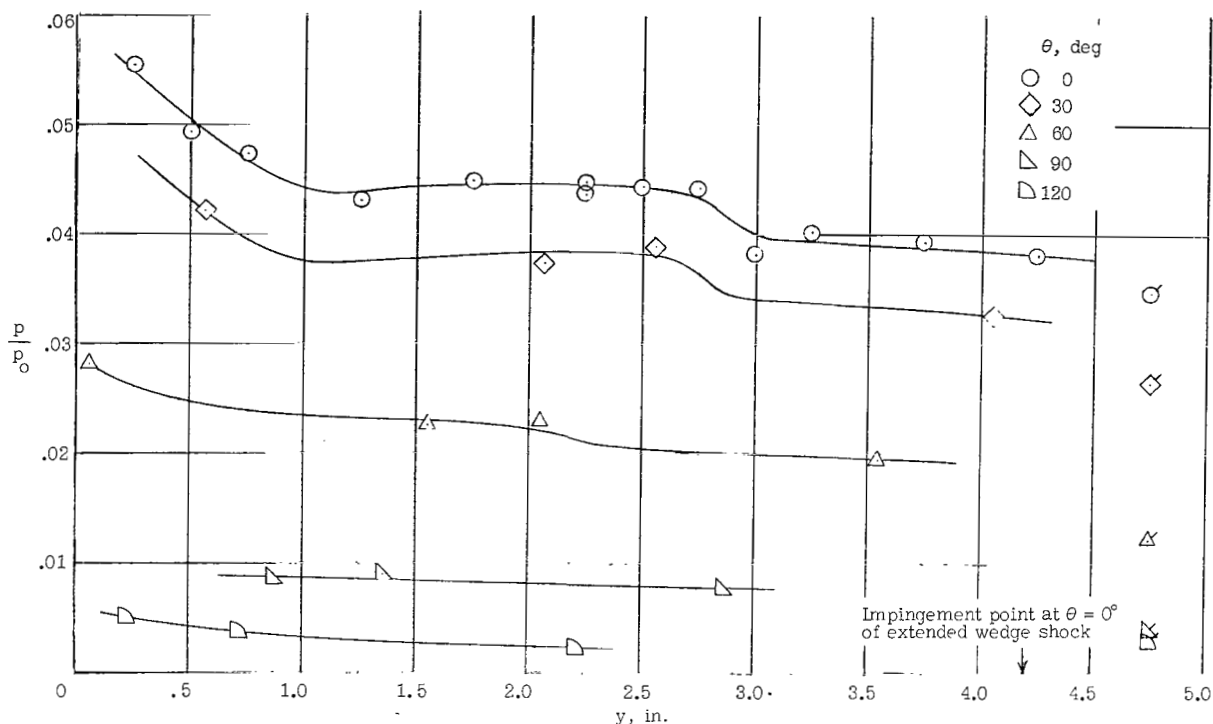
(b) Spanwise pressure distribution at several values of θ. Flagged symbols are measured pressures on an undisturbed cylinder from reference 2.

Figure 5.- Concluded.

This figure shows more clearly that a general rise in pressure occurs all along the cylinder from the station $y_s = 4.25$ inches, which is the greatest value of y_s for which data were obtained. The flagged symbols are the values measured in reference 2 and represent the pressures at a large distance from the wedge. For $\Lambda = 60^\circ$ the projected wedge shock would impinge on the cylinder at approximately $y_s = 4.2$ inches. Comparison of this value of y_s with the value $y_s = 1.15$ inches for $\Lambda = 20^\circ$ indicates that the large y extent of the pressure disturbance for $\Lambda = 60^\circ$ is largely a result of the geometry. Just as for $\Lambda = 20^\circ$, the pressure disturbance in the shock impingement region is small. The highest observed pressure again occurs close to the wedge, but for $\Lambda = 60^\circ$ there was evidently no drop in pressure closer to the wedge. This result possibly indicates that there was no separation in this area.

Schlieren

A schlieren photograph of the flow over the cylinder-wedge configuration is shown in figure 6. This figure confirms that for $\Lambda = 60^\circ$ there was no separation ahead of the base of the cylinder. The angle of the internal shock attached to the cylinder was measured as 31.3° with respect to the local wedge flow, as obtained from figure 7, which is a sketch, in scale, of the shock configuration

12

Figure 6.- Schlieren photograph of interference flow region on cylinder for $\Lambda = 60^O$, $\alpha = 8^O$, $l = 3.28$ inches, and $R_{\infty,D} = 2.08 \times 10^6$.

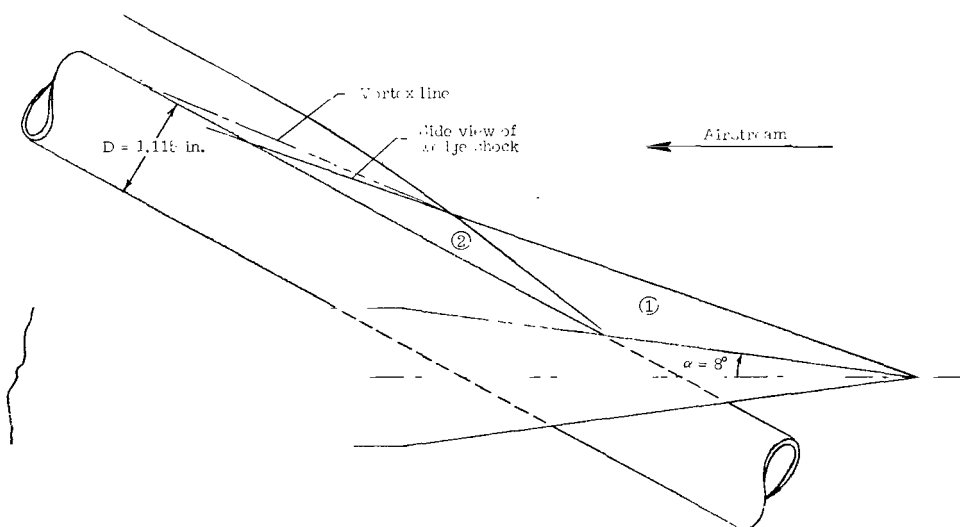Figure 7.- Sketch of schlieren for $\Lambda = 60^O$.

from figure 6. The computed stagnation-line pressure ratio for a cylinder assumed parallel to this internal shock would be $p_s/p_0 = 0.058$. The good agreement of this value with the peak measured value of 0.055 from figure 5(b) indicates that the flow on the cylinder in the immediate vicinity of the wedge can be calculated from the aforementioned assumption. The vortex line originating at the intersection of the wedge shock and cylinder bow shock (figs. 6 and 7) would impinge on the cylinder about 5 diameters along the stagnation line from the wedge, or at $y_s \approx 5.5$ inches. The pressures on the cylinder out to this value of y_s would therefore be larger than those on the undisturbed cylinder, as already indicated by the data shown in figure 5(b).

Heat Transfer

Heat-transfer coefficients and recovery temperatures were obtained from at least three runs made at different coolant temperatures but constant tunnel conditions as described in reference 2. The ratios of recovery temperature to stream-stagnation temperature generally decreased from the undisturbed values by 1 or 2 percent in the interference region. Even though this decrease is included in all heat-transfer-coefficient data reported, the recovery-temperature data are not reported because the small observed decreases were almost within the range of experimental errors.

$\Lambda = 20^\circ$.- The heat-transfer distribution on the cylinder for $\Lambda = 20^\circ$ with the 8° half-angle wedge is presented in figure 8. Figure 8(a) shows that at
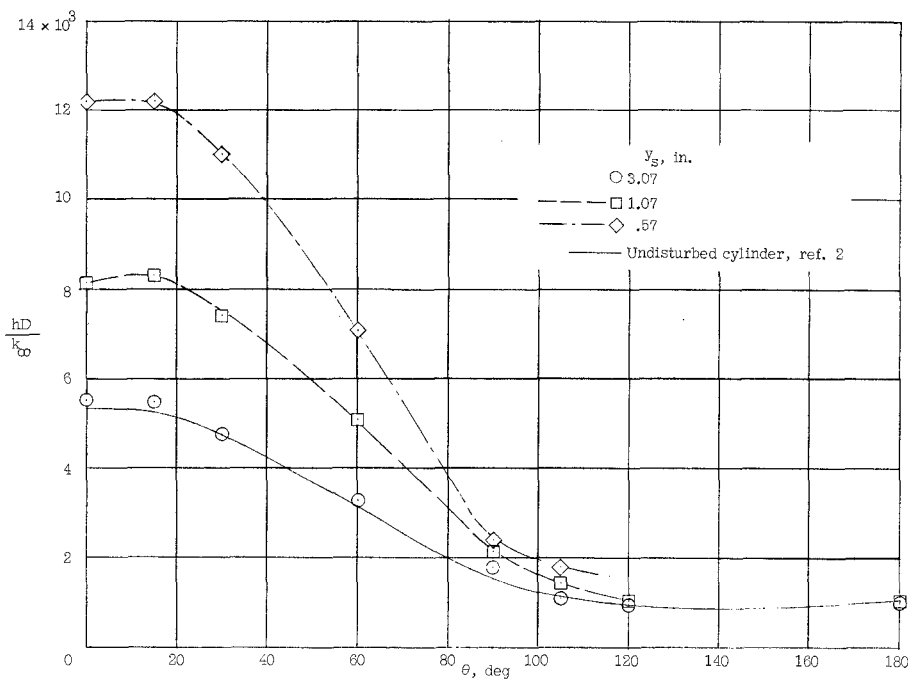
(a) Chordwise Nusselt number variation at three spanwise stations, $R_{\infty,D} = 1.56 \times 10^6$. Faired curve is from experimental data of reference 2 adjusted to this Reynolds number.

Figure 8.- Heat-transfer distribution on cylinder for $\Lambda = 20^\circ$, $\alpha = 8^\circ$, and $l = 4.16$ inches.

14

$y_s = 3.07$ inches the Nusselt number distribution is essentially the same as the undisturbed distribution measured in reference 2. As the wedge is approached, the Nusselt number over the entire forward section of the cylinder increases by about the same percentage increases as for the pressures given in figure 2(a). The same data are plotted against y in figure 8(b) as the ratio of h/h_{inf} where h_{inf} is the measured heat-transfer coefficient on an undisturbed cylinder from reference 2, adjusted to the appropriate value of $R_{\infty,D}$. Here again the trend in heat-transfer distribution is similar to the trend in pressures of figure 2(b). Note that the peak heating is well inboard of the shock-impingement region, which from figure 3 would be at $y_s \approx 1.15$ inches. The distribution of heat-transfer coefficients along the stagnation line of the cylinder with the 8° wedge is compared with the distribution obtained with the flat plate in
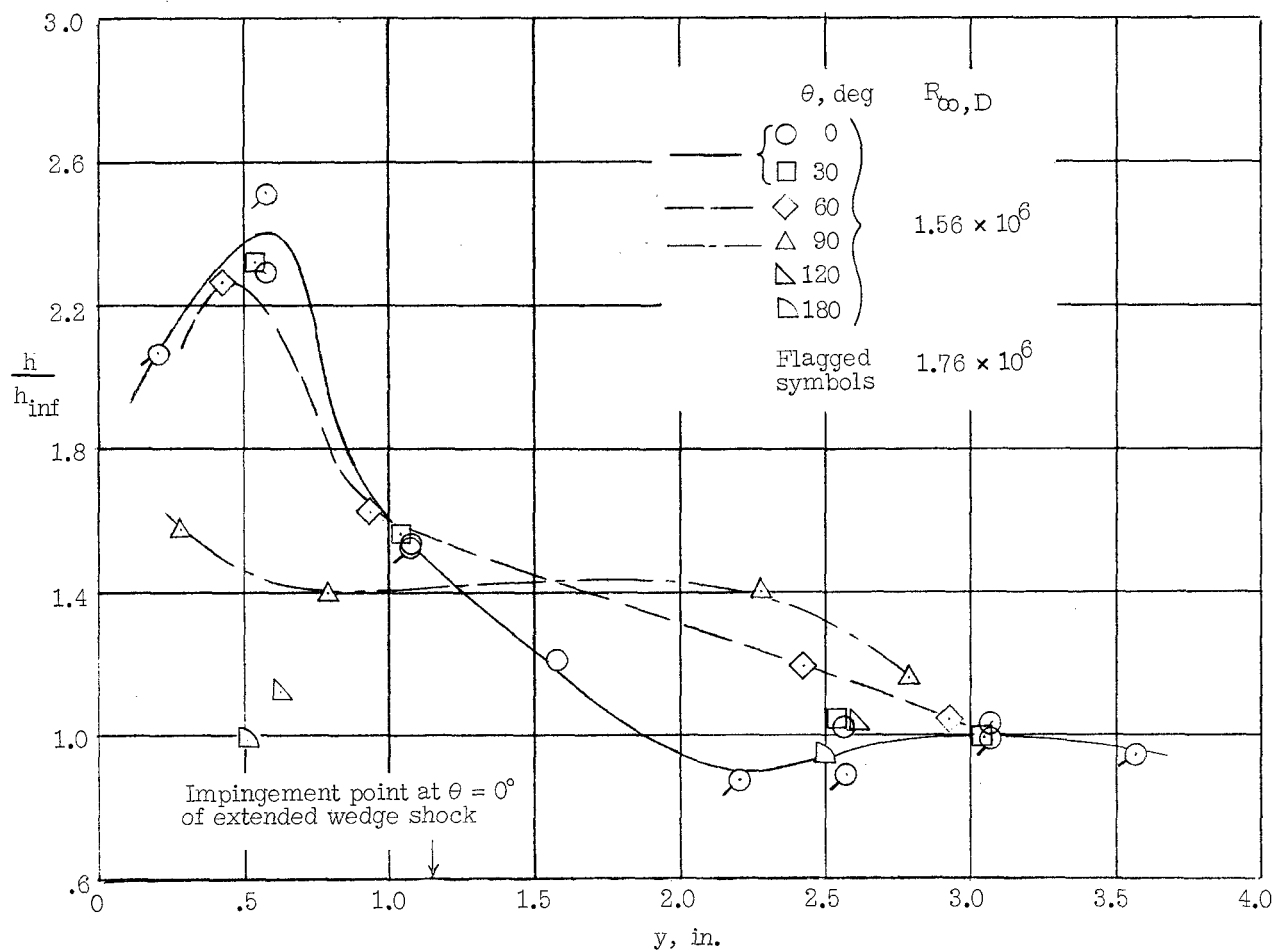
(b) Spanwise distribution of heat-transfer coefficient at several values of θ and two Reynolds numbers.

Figure 8.- Concluded.

figure 9. The trends are similar, but the peak heating ratio caused by the plate is only about 1.3 as compared with 2.5 for the wedge.
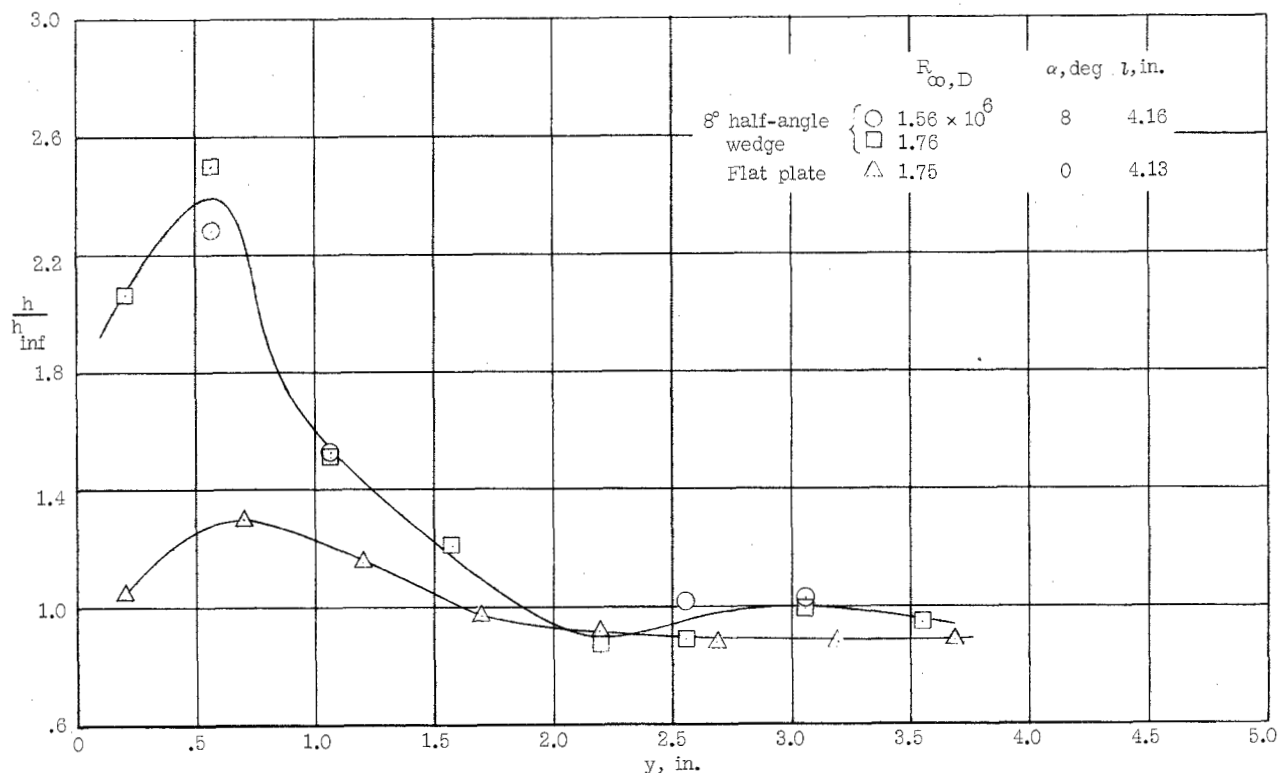

Figure 9.- Effect of wedge angle on the spanwise distribution of heat-transfer coefficient at stagnation line of cylinder for $\Lambda = 20^\circ$ and $l = 4.16$ inches.

The local effective conditions just upstream of the cylinder on the wedge (or plate) are sufficient to account for the peak heating as indicated by the following considerations. Equation (2) of reference 2 was used to compute turbulent heating on the cylinder with the following conditions: (1) the effective sweep angle was taken as $\Lambda = 28^\circ$ for the wedge and $\Lambda = 20^\circ$ for the plate; (2) the measured peak pressures from figure 4 ($p_S/p_O = 0.25$ for the wedge and $p_S/p_O = 0.19$ for the plate), together with the computed local flow conditions on the wedge or plate (with $R_{\infty,D} = 1.76 \times 10^6$), were used as the effective upstream values; and (3) the reference value h_{inf} was computed by the same method but for $\Lambda = 20^\circ$, $M_\infty = 4.15$, and $R_{\infty,D} = 1.76 \times 10^6$. The results of this calculation are as follows:

	Computed h/h_{inf}	Measured h/h_{inf}
For 8° wedge	2.40	2.50
For flat plate	($l = 1.57$ in.) 1.56	($l = 4.13$ in.) 1.30

16

The good agreement between the computed and measured values for the 8° wedge indicates that the assumptions for the flow conditions are probably valid. The agreement for the flat plate is not as good, possibly because the correct pressure ratio for the longer flat plate (see fig. 4) was not available. It should be emphasized that the experimental and theoretical reference or undisturbed values are essentially turbulent; thus, the situation is not complicated by any transitional effects.

The effect of Reynolds number on h/h_{inf} for $\Lambda = 20^{\circ}$ at one spanwise station is shown in figure 10. Up to $\theta = 30^{\circ}$, the effect is small; but from $\theta = 60^{\circ}$ to 120°, the values of h/h_{inf} are larger at the smaller Reynolds number.
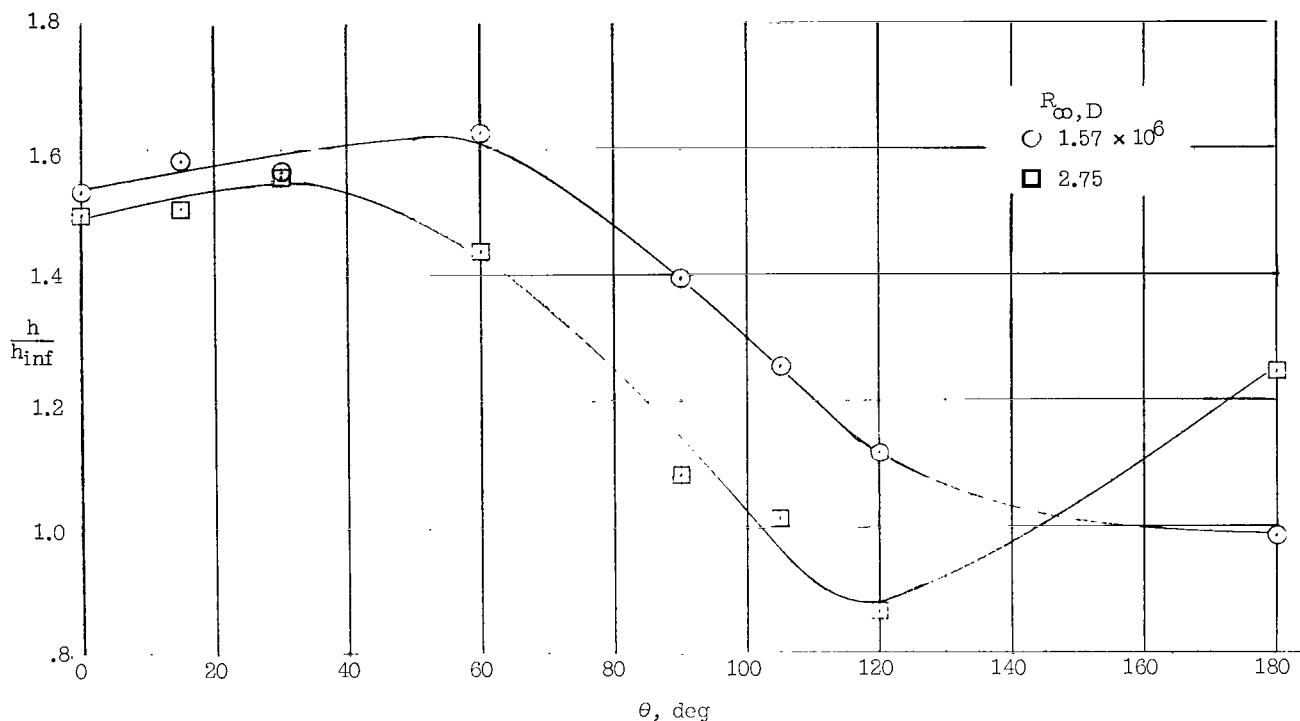

Figure 10.- Effect of Reynolds number on heat-transfer-coefficient ratio for $\Lambda = 20^{\circ}$, $y_s = 1.07$ inches, $\alpha = 8^{\circ}$, and $l = 4.16$ inches.

Heat-transfer distribution data for $\Lambda = 60^{\circ}$ with an 8° wedge are shown in figure 11. The distributions at several angular locations θ, as well as the stagnation-line distribution at $\theta = 0^{\circ}$, are included. Here again the heat-transfer ratios are largest near the wedge, and the effect of the shock itself, which would impinge at some distance outboard as indicated in figure 7, is negligible. The peak increases in this case are smaller than for $\Lambda = 20^{\circ}$. The analysis procedure used for $\Lambda = 60^{\circ}$ was modified slightly to take advantage of the schlieren data (figs. 6 and 7). The flow on the wedge is computed by using the measured wedge-shock angle of 20.2°. The effective yaw angle used in the

17

2.6

2.2

1.8

$\dfrac{h}{h_{inf}}$

1.4

1.0

.6

0   .5   1.0   1.5   2.0   2.5   3.0   3.5   4.0   4.5   5.0

y, in.

θ, deg
○   0
☐   30
◇   60
△   90
◻ 120

Impingement point at $\theta = 0°$
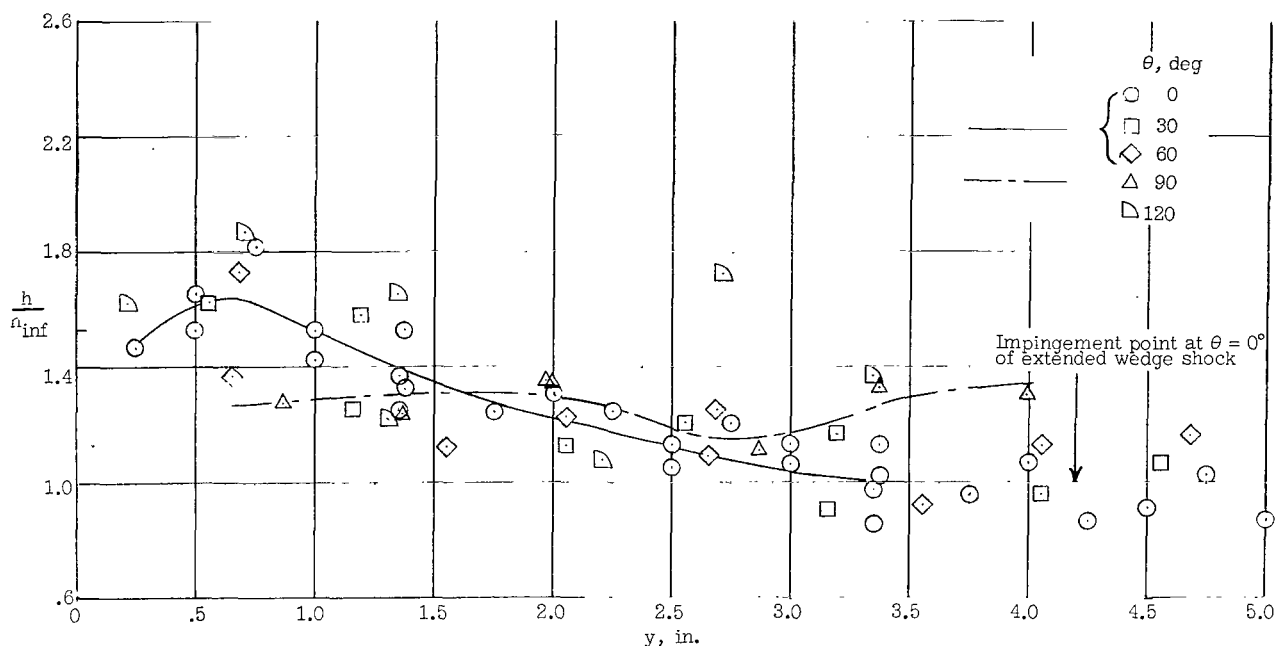of extended wedge shock

Figure 11.- Effect of 8° half-angle wedge on heat-transfer coefficient on cylinder for several values of θ with $\Lambda = 60°$, $R_{\infty,D} = 1.6 \times 10^6$, and $l = 3.28$ inches.

calculation for the cylinder was taken as

$$60° + 8° - 9.3° = 58.7°$$

where the 8° corrects for the local flow on the wedge and the -9.3° corrects for the shock wave generated by the cylinder within the wedge flow field. That is, for the purpose of this calculation, the cylinder was assumed to be yawed at the same angle as this internal shock with respect to the local wedge flow as discussed previously in regard to the peak pressure. (This procedure resulted in a computed value of $p_s/p_o = 0.058$ compared with the measured value of $p_s/p_o = 0.055$ from fig. 5(b).) The reference value h_{inf} is again the turbulent value for an undisturbed cylinder at the same free-stream conditions. The result of this calculation is $h/h_{inf} = 1.53$, compared to the peak measured value of $h/h_{inf} \approx 1.64$ from the faired curve of figure 11. Thus, in this case, in which there is no separation or transition, both the increased heating and pressure can be accounted for by using local effective flow values and by treating the attached shock at the base of the cylinder as the cylinder bow shock.

CONCLUDING REMARKS

The general pattern which emerges from the analysis of the present data, together with previous results, is first that an impinging shock wave, as such, does not cause a local increase in heating on a leading edge. Rather, the

impinging shock wave, together with the interference effects at the root of the leading edge, causes transition in the inherently unstable boundary layer on a swept leading edge. Secondly, the peak heating can be predicted by using the local flow conditions upstream of the intersection region in the theory for turbulent heating on a yawed cylinder. If there is no separation ahead of the leading edge, the stagnation-line pressure required in the theory is calculated by assuming a shock attached at the root line. When separation is present, measured cylinder pressures should be used in the theory. If measured pressures are not available, a reasonable estimate of the peak heating can be obtained by using a leading-edge pressure intermediate between the values for an attached shock and isentropic compression.

The results of the present investigation indicate that for sufficiently large Reynolds numbers and sweep angles, separation at the root of the cylinder does not occur. For smaller sweep angles, separation may occur with a resulting large increase in pressure and heat transfer near the supporting body. The measured pressure for this latter situation is between the extremes that would exist for an attached shock and isentropic compression of the local wedge flow.

Transition to turbulent boundary layer was not a factor in the increased heating observed in the present tests, since turbulent boundary layers were already present for comparable conditions on an undisturbed cylinder. Therefore, the peak increases in heating could be predicted accurately with turbulent theory, if appropriate local flow conditions were used.

Langley Research Center,
    National Aeronautics and Space Administration,
        Langley Station, Hampton, Va., January 16, 1964.

REFERENCES

1. O'Neal, Robert L., and Bond, Aleck C.: Heat Transfer to 0° and 75° Swept Blunt Leading Edges in Free Flight at Mach Numbers From 1.90 to 3.07. NASA TN D-1256, 1962. (Supersedes NACA RM L58A13.)

2. Beckwith, Ivan E., and Gallagher, James J.: Local Heat Transfer and Recovery Temperatures on a Yawed Cylinder at a Mach Number of 4.15 and High Reynolds Numbers. NASA TR R-104, 1961.

3. Chapman, Gary T.: Some Effects of Leading-Edge Sweep on Boundary-Layer Transition at Supersonic Speeds. NASA TN D-1075, 1961.

4. Burbank, Paige B., Newlander, Robert A., and Collins, Ida K.: Heat-Transfer and Pressure Measurements on a Flat-Plate Surface and Heat-Transfer Measurements on Attached Protuberances in a Supersonic Turbulent Boundary Layer at Mach Numbers of 2.65, 3.51, and 4.44. NASA TN D-1372, 1962.

5. Newlander, Robert A.: Effect of Shock Impingement on the Distribution of Heat-Transfer Coefficients on a Right Circular Cylinder at Mach Numbers of 2.65, 3.51, and 4.44. NASA TN D-642, 1961.

6. Jones, Robert A.: Heat-Transfer and Pressure Investigation of a Fin-Plate Interference Model at a Mach Number of 6. NASA TN D-2028, 1964.

7. Carter, Howard S., and Carr, Robert E.: Free-Flight Investigation of Heat Transfer to an Unswept Cylinder Subjected to an Incident Shock and Flow Interference From an Upstream Body at Mach Numbers up to 5.50. NASA TN D-988, 1961.

NASA SCIENTIFIC AND TECHNICAL PUBLICATIONS

TECHNICAL REPORTS: Scientific and technical information considered important, complete, and a lasting contribution to existing knowledge.

TECHNICAL NOTES: Information less broad in scope but nevertheless of importance as a contribution to existing knowledge.

TECHNICAL MEMORANDUMS: Information receiving limited distribution because of preliminary data, security classification, or other reasons.

CONTRACTOR REPORTS: Technical information generated in connection with a NASA contract or grant and released under NASA auspices.

TECHNICAL TRANSLATIONS: Information published in a foreign language considered to merit NASA distribution in English.

TECHNICAL REPRINTS: Information derived from NASA activities and initially published in the form of journal articles.

SPECIAL PUBLICATIONS: Information derived from or of value to NASA activities but not necessarily reporting the results of individual NASA-programmed scientific efforts. Publications include conference proceedings, monographs, data compilations, handbooks, sourcebooks, and special bibliographies.

Details on the availability of these publications may be obtained from:

SCIENTIFIC AND TECHNICAL INFORMATION DIVISION
NATIONAL AERONAUTICS AND SPACE ADMINISTRATION
Washington, D.C. 20546